WALAILAK JOURNAL

http://wjst.wu.ac.th

MiniReview

Mathematical Models of Bead-Spring Jets during Electrospinning for Fabrication of Nanofibers

Thananchai DASRI*

Faculty of Applied Science and Engineering, Nong Khai Campus, Khon Kaen University, Nong Khai 43000, Thailand

(*Corresponding author; e-mail: thananchai_dasri@hotmail.com)

Received: 22 July 2012, Revised: 29 October 2012, Accepted: 26 November 2012

Abstract

Electrospinning is a popular technique to produce structures in the form of nanofibers. These nanofibers can be used for many applications such as filtration composites, insulator and energy storage. The technique is based on the electrostatic force that acts on the polymeric solution. However, during the electrospinning process the liquid jet shows unstable behavior. This problem causes the random formation of nanofibers. This article focuses on the mathematical models to describe the dynamics behavior of the fluid jet in the electrospinning process. There are a lot of different parameters in the model. Variation in these parameters results in a change in jet behaviors. This brief review is a summary of the authors' recent work. The Reneker's model and Wu's model are used to describe the dynamics behavior of the jet used in electrospinning.

Keywords: Nanofibers, electrospinning, mathematical model, magneto-electrospinning

Introduction

Electrospinning is a process for fabricating nanofibers from a polymeric solution or melt using strong electrical field energy as seen in **Figure 1**. Electrospun nanofibres have interesting properties such as high-specific surface area, high porosity, high absorption capacity, all of which are useful properties for applications. Thus, there are many potential applications of fibers in a variety of areas like composites, biotechnology, environmental engineering, defense, optics and electronics that have been discovered [1-17]. The process of electrospinning involves three stages that correspond to the electrospun jet behavior. The first stage is the formation of a Taylor cone. Next is the formation of a straight jet. The last stage after moving to a specific position of its path, a bending instability usually occurs farther downstream. Therefore, there are many research groups that theoretically study fiber formation. Two main models have emerged to describe the jet behavior during electrospinning. The stable jet is considered as a slender model, proposed by Spivak *et al*. [18,19], Hohman *et al*. [20,21] and Feng [22,23]. The second jet model, called the instability model, is studied by Reneker *et al*. [24,25] and Theron *et al*. [26]. Spivak *et al*. [17,18] developed an electrohydrodynamic model of steady state electrospinning in a single jet regime, and considered power-law fluid behavior. Governing equations consist of mass balance, linear momentum balance, and electric charge balance. Hohman *et al*. [20,21] later proposed a model that the interaction of the surface charges in the jet with the external applied electric field plays an important role in the jet development. However, only Newtonian fluids were considered.

In the instability model, the jet is considered to consist of a series of discrete elements (charged beads) connected by dumbbell elements [24-27]. This model was improved and expanded by Wu *et al*. [28]. They proposed a very effective method called magneto-electrospinning to control the instability phenomena in electrospinning. This model later was numerically studied by Xu *et al*. [29].

In this paper, the mathematical model of only the instability stage is reviewed. The governing equations are thus based upon the Reneker *et al*. [24] and Wu *et al*. [28] models.

Electrospinning process

A schematic diagram of the electrospinning process is shown in **Figure 1**. Many previous researchers have used an apparatus similar to the one given in **Figure 1** [24,26,29-30]. The apparatus has three major components: a high voltage power supply, a spinneret (which is a metallic needle) and collector plate (a grounded conductor). In the system, a high voltage power supply is connected to an electrode immersed in the reservoir and a collector plate located some distance for supplying the electric potential between the two. As the electric potential slowly increases to several kV (kilovolts), the drop begins to change shape and looks more like a cone known as a Taylor cone. When the potential has reached a critical value, a liquid jet is extracted from the nozzle and accelerated towards a grounded collecting substrate.

Governing parameters

To understand the mathematical model, first the effects of these parameters on morphology and diameter of electrospun nanofibres will be presented. There are three parameters which can be manipulated in the electrospinning. These are solution properties, processing conditions and ambient parameters. The solution properties are the type of polymer and solvent, polymer molecular weight, viscosity (or concentration), surface tension, elasticity and electrical conductivity. The processing conditions are the feed rate of the polymer solution, the spinneret to collector separation distance, the inner diameter of the needle, the type of collector and the strength of the applied voltage. The ambient parameters are temperature and humidity. Many experimental studies have reported these parameters [30-41]. For instance, Son *et al*. [31] reported that, the average diameter of poly(ethylene oxide) (PEO) nanofibres decrease with increasing PEO solution conductivity and solvent polarity. They also revealed that, the average diameter of cellulose acetate (CA) nanofibres was not significantly changed by changing operating parameters, but increases by increasing CA solution concentration [32]. Fong *et al*. [33] observed the formation of electrospun beaded nanofibers. They found that the solution viscosity, net charge density carried by the electrospinning jet and surface tension of the solution are the main factors. Wannatong *et al*. [34] showed that, in electrospinning of polystyrene (PS) solutions, at first the fibre diameters slightly decrease with increasing applied voltage, and then increase with a further increase in the applied voltage. Vrieze *et al*. [39] studied the role of temperature and humidity on electrospinning. They reported that increasing ambient humidity decreases the diameter of polyethylene oxide (PEO) and finally results in beaded fibres. Wang *et al*. [40] reported that, the temperature affects the cone/jet/fiber morphologies as well as the birefringence and crystallinity of the collected PAN fibers. In recently reported work, Wu *et al*. [28] proposed an electrospinning system for controlling stability of the electrospun fiber by applying a magnetic field. Later, Xu *et al*. [29] analyzed numerically the effect of the magnetic field on electrospinning. When they applied a magnetic field in the electrospinning they found that the problem of bending instability can be completely overcome.

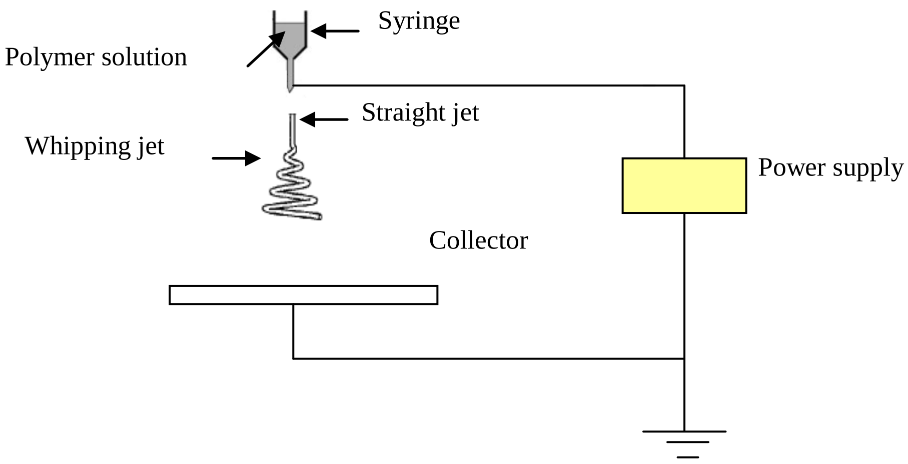

Figure 1 Schematic diagram of the electrospinning process.

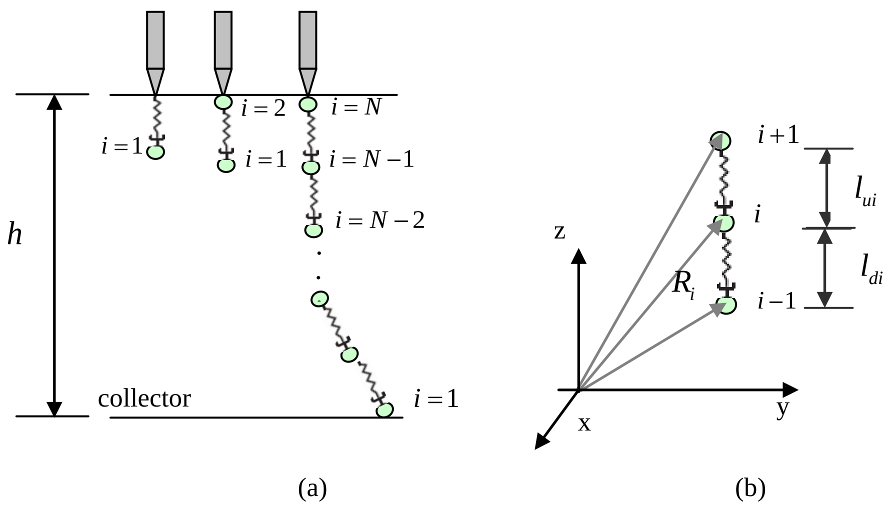

Figure 2 The schematic of the computational model. The jet is supposed to be composed of a series of electrically charged beads. (a) Charged bead moves downward to the collector. (b) Location of *i*, *i*+1 and *i*-1 bead.

Mathematical model

A schematic diagram of the electrospinning process is shown in **Figure 1** [24]. The apparatus has three major components: a high voltage power supply, a spinneret (which is a metallic needle) and collector plate (a grounded conductor). The notations presented in this article are provided in **Table 1**.

Table 1 Symbols employed and their definitions.

Symbol	Definition	Units (in cgs)
q	charge	$(g^{1/2}cm^{3/2})/s$
a	cross-section radius	cm
a_o	initial cross-section radius	cm
γ	surface tension of the solution	g/s^2
m	mass	g
V_o	voltage	$(g^{1/2}cm^{1/2})/s$
G	elastic modulus	$g/(cm\ s^2)$
σ	stress	$g/(cm\ s^2)$
ω	frequency of the perturbation	s^2
l	length of the ideal rectilinear jet	cm
L	length scale	cm
t	time	s
μ	viscosity	g/(cm s)
h	distance from pendent drop to grounded collector	cm

To describe the jet behavior, Reneker *et al.*'s model is employed. The model treats the jet as a series of beads connected together by viscoelastic dumbbells as shown in **Figure 2**. Each bead has a mass m and possesses a charge e. According to Newton's second law, each bead is acted on by Coulomb forces, electric field, viscoelastic, and surface tension forces. So, the equation of motion of the beads is

$$\frac{d^2}{dt^2}\vec{r}_i = \frac{1}{m}(\vec{F}_C + \vec{F}_E + \vec{F}_{ve} + \vec{F}_{sf}), \tag{1}$$

where m is the mass of the bead, F_C is the Coulombic force interaction between the i-th bead and the rest of the beads in the system, F_E is the electric field force imposed on bead i created by the potential difference between the capillary tip and the collector plate, F_{ve} is the viscoelastic force acting on bead i, and F_{sf} is the surface tension force acting on bead i. The Coulombic force is

$$\vec{F}_C = \sum_{\substack{j=1\\ j\neq i}}^{N} \frac{e^2}{R_{ij}^3}[(x_i - x_j)\hat{i} + (y_i - y_j)\hat{j} + (z_i - z_j)\hat{k}], \tag{2}$$

where $\hat{i}, \hat{j}$ and $\hat{k}$ are the unit vectors along the x, y, and z axes, respectively, and

$$R_{ij} = [(x_i - x_j)^2 + (y_i - y_j)^2 + (z_i - z_j)^2]^{\frac{1}{2}}. \tag{3}$$

The electric field force is

$$\vec{F}_E = -e\frac{V_0}{h}\hat{k}, \tag{4}$$

Where V_0 is the electric voltage, and h is distance between the pendent drop and the collector. The viscoelastic force is

$$\begin{aligned}\vec{F}_{ve} = {} & \frac{\pi a_{i,i+1}^2 \sigma_{i,i+1}}{l_{i,i+1}}[(x_{i+1} - x_i)\hat{i} + (y_{i+1} - y_i)\hat{j} + (z_{i+1} - z_i)\hat{k}] \\ & - \frac{\pi a_{i-1,i}^2 \sigma_{i-1,i}}{l_{i-1,i}}[(x_i - x_{i-1})\hat{i} + (y_i - y_{i-1})\hat{j}(z_i - z_{i-1})\hat{k}]\end{aligned}, \tag{5}$$

where $\sigma_{i-1,i}$ is the stress which pulls the bead of i back to $i-1$, while $\sigma_{i,i+1}$ is the stress which pulls the bead i forward to $i+1$. These stresses can be calculated by integrating the following equation,

$$\frac{d\sigma_{i,i+1}}{dt} = G\frac{1}{l_{i,i+1}}\frac{d}{dt}l_{i,i+1} - \frac{G}{\mu}\sigma_{i,i+1}, \quad (6)$$

$$\frac{d\sigma_{i-1,i}}{dt} = G\frac{1}{l_{i-1,i}}\frac{d}{dt}l_{i-1,i} - \frac{G}{\mu}\sigma_{i-1,i}, \quad (7)$$

where t is time, G, μ, and l are the connector element elastic modulus, viscosity, and length, respectively. $\frac{d}{dt}l_{i,i+1}$ is the rate of strain of bead i and $i+1$, while $\frac{d}{dt}l_{i-1,i}$ is the rate of strain of bead i and $i-1$. The rate of strains are calculated by using the following equation,

$$\frac{d}{dt}l_{i,i+1} = \frac{1}{l_{i,i+1}}[(x_{i+1}-x_i)\times\dot{x}_{i+1} + (-x_{i+1}+x_i)\times\dot{x}_i + (y_{i+1}-y_i)\times\dot{y}_{i+1} + (-y_{i+1}+y_i)\times\dot{y}_i + (z_{i+1}-z_i)\times\dot{z}_{i+1} + (-z_{i+1}+z_i)\times\dot{z}_i] \quad (8)$$

$$\frac{d}{dt}l_{i-1,i} = \frac{1}{l_{i-1,i}}[(x_i-x_{i-1})\times\dot{x}_i + (-x_i+x_{i-1})\times\dot{x}_{i-1} + (y_i-y_{i-1})\times\dot{y}_i + (-y_i+y_{i-1})\times\dot{y}_{i-1} + (z_i-z_{i-1})\times\dot{z}_i + (-z_i+z_{i-1})\times\dot{z}_{i-1}] \quad (9)$$

The filament radii $a_{i-1,i}$ and $a_{i,i+1}$ can be calculated from mass conservation and neglecting the solution evaporation,

$$a_{i,i+1} = a_o\sqrt{\frac{L}{l_{i,i+1}}}, \quad (10)$$

$$a_{i-1,i} = a_o\sqrt{\frac{L}{l_{i-1,i}}}, \quad (11)$$

where $L = \sqrt{\frac{4e^2}{\pi a_0^2 G}}$ is defined as the length scale and a_0 is the initial jet diameter at *t*=0, $l_{i-1,i}$ and $l_{i,i+1}$ are the segment length. These distances are given by the following equation.

$$l_{i,i+1} = [(x_{i+1}-x_i)^2 + (y_{i+1}-y_i)^2 + (z_{i+1}-z_i)^2]^{\frac{1}{2}}, \quad (12)$$

$$l_{i-1,i} = [(x_i-x_{i-1})^2 + (y_i-y_{i-1})^2 + (z_i-z_{i-1})^2]^{\frac{1}{2}}. \quad (13)$$

and the surface tension force is

$$\vec{F}_{sf} = -\frac{\alpha\pi(a^2)_{av}K_i}{(x_i^2+y_i^2)^{\frac{1}{2}}}(|x_i|\,\mathrm{sign}(x_i)\hat{i} + |y_i|\,\mathrm{sign}(y_i)\hat{j}], \quad (14)$$

where α is the surface tension coefficient, K_i is the curvature of jet segment of $i-1$ and $i+1$. The average jet radius is defined as follows:

$$(a^2)_{avg} = \frac{(a_{i,i+1} + a_{i-1,i})^2}{4}, \quad (15)$$

The meaning of "sign" in Eq. (14) is as follows:

$$\text{sign}(x) = \begin{cases} 1, & \text{if } x > 0, \\ 0, & \text{if } x = 0, \\ -1, & \text{if } x < 0, \end{cases} \quad (16)$$

By substituting Eq. (2), Eq. (4), Eq. (5) and Eq. (14) into Eq. (1), it can be rewritten separately in terms of the x, y and z directions as follows,

$$\frac{d^2}{dt^2} x_i = \frac{1}{m}[\sum_{\substack{j=1 \\ j\neq i}}^{N} \frac{e^2}{R^3_{\ ij}}(x_i - x_j) + \frac{\pi a^2_{i,i+1}\sigma_{i,i+1}}{l_{i,i+1}}(x_{i+1} - x_i) - \frac{\pi a^2_{i-1,i}\sigma_{i-1,i}}{l_{i-1,i}}(x_i - x_{i-1}) - \frac{\alpha\pi(a^2)_{av} K_i}{(x_i^2 + y_i^2)^{\frac{1}{2}}}(|x_i| \text{sign}(x_i))], \quad (17)$$

$$\frac{d^2}{dt^2} y_i = \frac{1}{m}[\sum_{\substack{j=1 \\ j\neq i}}^{N} \frac{e^2}{R^3_{\ ij}}(y_i - y_j) + \frac{\pi a^2_{i,i+1}\sigma_{i,i+1}}{l_{i,i+1}}(y_{i+1} - y_i) - \frac{\pi a^2_{i-1,i}\sigma_{i-1,i}}{l_{i-1,i}}(y_i - y_{i-1}) - \frac{\alpha\pi(a^2)_{av} k_i}{(x_i^2 + y_i^2)^{\frac{1}{2}}} * (|y_i| \text{sign}(y_i))] \quad (18)$$

and

$$\frac{d^2}{dt^2} z_i = \frac{1}{m}[\sum_{\substack{j=1 \\ j\neq i}}^{N} \frac{e^2}{R^3_{\ ij}}(z_i - z_j) - e\frac{V_0}{h} + \frac{\pi a^2_{i,i+1}\sigma_{i,i+1}}{l_{i,i+1}}(z_{i+1} - z_i) - \frac{\pi a^2_{i-1,i}\sigma_{i-1,i}}{l_{i-1,i}}(z_i - z_{i-1}). \quad (19)$$

Additionally, in the calculation the air drag force and gravity force are neglected. As both space and time are dependent perturbations. Therefore the development of whipping instability occurs. To model this, a single perturbation is added by inserting an initial bead of *i* by

$$x_i = 10^{-3} L \sin(\omega t),$$

$$y_i = 10^{-3} L \cos(\omega t), \quad (20)$$

where ω is the perturbation frequency.

Recently, Wu *et al*. [28] proposed a very effective method called magneto-electrospinning to control the instability phenomena in electrospinning. In this new method a magnetic field is applied in the process, as shown in **Figure 3**.

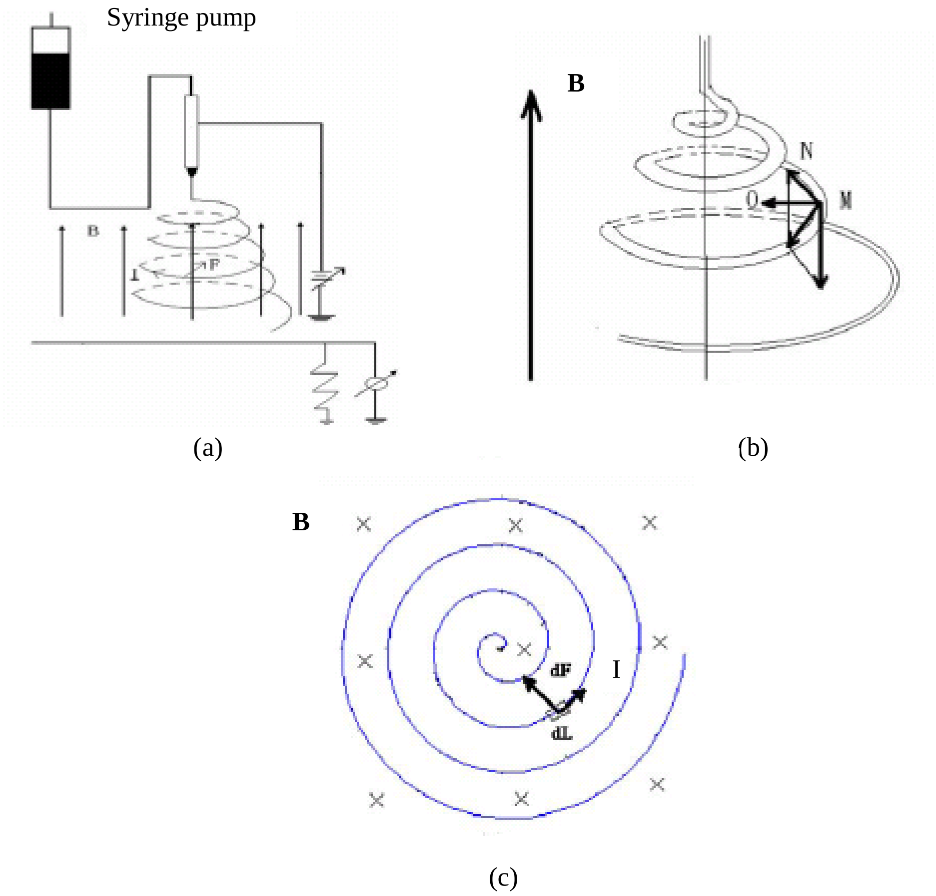

Figure 3 Schematic diagram of the magneto-electrospinning process [28]. (a) Magnetic field in the electrospinning process, (b) The result of magnetic field in an electrospun jet and (c) Ampere force in the electronic jet when a magnetic field is applied.

In addition the current numerical model has been studied by Xu *et al*. [29]. They defined the equation of motion as follows:

$$\frac{d^2}{dt^2}\bar{\mathrm{r}}_{\mathrm{i}} = \frac{1}{m}(\bar{\mathrm{F}}_{\mathrm{C}} + \bar{\mathrm{F}}_{\mathrm{E}} + \bar{\mathrm{F}}_{\mathrm{ve}} + \bar{\mathrm{F}}_{\mathrm{cap}} + \bar{\mathrm{F}}_{\mathrm{B}}), \tag{21}$$

where $\bar{\mathrm{F}}_B$ is defined as

$$\bar{\mathrm{F}}_{\mathrm{B}} = qB\frac{dy_i}{dt}\hat{\mathrm{i}} + qB\frac{dx_i}{dt}\hat{\mathrm{j}}, \tag{22}$$

where B is the magnetic induction.

According to the mathematical model described above, the jet simulation proceeds as follows [28]: first of all, at t = 0, the initial whipping jet includes two beads, bead 1 and bead 2. The distance $l_{1,2}$ is set to be a small distance, say, h/50000. Other initial conditions, including the stresses $\sigma_{i-1,i}$ and $\sigma_{i,i+1}$, and the initial velocity of the bead i, $\frac{d\bar{\mathrm{r}}_{\mathrm{i}}}{dt}$, are set to be zero. For a given time t when the last bead is pulled out of the pendent drop the new bead say, $i = N$, is added at the upper end of the jet. While the distance between this bead and the pendent drop becomes long enough, say, $\frac{h}{25000}$, a new bead of $i = N + 1$ is inserted at a small distance, $\frac{h}{50000}$, from the previous one. At the same time a small perturbation is added to its *x* and *y* coordinates, defined in Eq. (20). Eventually, by numerically solving of Eq. (17) - Eq. (19) the configuration of the jet in evolutionary time is obtained.

According to the mathematical model presented above, the electrospun jet is considered to be a series of discrete charged beads connected by a viscoelastic spring. A major advantage of this model is that the discretization of the jet allows the trajectory of the bending instability to be followed as it develops. The trajectories appeared from this model are similar in character to those observed experimentally [24]. Another interesting model, called the continuum-type model, is also used to analyze the jet profile [17-22]. In this model the jet momentum equation (including a term for the electrical force on the jet), jet continuity equation and electric field equation are coupled together. The onset of the whipping instability in this analysis is allowed to be examined under the assumption that the fluids are Newtonian. Recently, He *et al*. [42] suggested that at the nanoscale there is the nano-effect arising similar to that in the quantum world. A new theory so should be developed link both Newtonian mechanics and quantum mechanics. They advised that the new theory might incorporate El Naschie's E-infinite theory [43-45]**.**

Conclusions

This article has reviewed the mathematical models for developing the electrospinning process. The Reneker and Wu's two-part models are used to describe the dynamics behavior of the electrospun jet. The forces acting on the jet in the Reneker's model are Coulombic, electric field, viscoelastic and surface tension forces. The result of the bending instability phenomenon, the magnetic field so is applied to control instability which was proposed by Wu's model.

Acknowledgements

This work is supported by the Foundation for the new completed PhD lecturer of Khon Kaen University (KKU). So, I would like to thank Khon Kaen University for this financial support. I would like to thank for all for performing this work.

References

[1] PR Kumar, N Khan, S Vivekanandhan, N Satyanarayana, AK Mohanty and M Misra. Nanofibers: effective generation by electrospinning and their applications. *J. Nanosci. Nanotechnol.* 2012; **12**, 1-25.

[2] WE Teol and S Ramakrishna. A review on electrospinning design and nanofibre assemblies. *Nanotechnology* 2006; **17**, R89-R106.

[3] XH Qin and SY Wang. Electrospun nanofibers from crosslinked poly(vinyl alcohol) and its filtration efficiency. *J. Appl. Polym. Sci.* 2008; **109**, 951-6.

[4] JD Schiffman and CL Schauer. One-step electrospinning of cross-linked chitosan fibers. *Biomacromolecules* 2007; **8**, 2665-7.

[5] T Subbiah, GS Bhat, RW Tock, S Pararneswaran and SS Ramkumar. Electrospinning of nanofibers. *J. Appl. Polym. Sci.* 2005; **96**, 557-69.

[6] M Naebe, T Lin, MP Staiger, LM Dai and XG Wang. Electrospun single-walled carbon nanotube/polyvinyl alcohol composite nanofibers: structure-property relationships. *Nanotechnology* 2008; **19**, 305702.

[7] SJ Lee, JJ Yoo, GJ Lim, A Atala and Stitze. *In vitro* evaluation of electrospun nanofiber scaffolds for vascular graft application. *J. Biomed. Mater. Res. Part A* 2007; **83A**, 999-1008.

[8] P Heikkila, A Taipale, M Lehtimaki and A Harlin. Electrospinning of polyamides with different chain compositions for filtration application. *Polym. Eng. Sci.* 2008; **48**, 1168-76.

[9] MM Munir, F Iskandar, Khairurrijal and K Okuyama1. A constant-current electrospinning system for production of high quality nanofibers. *Rev. Sci. Instrum.* 2008; **79**, 093904.

[10] C Huang, S Chen, C Lai, DH Reneker, H Qiu, Y Ye and H Hou. Electrospun polymer nanofibres with small diameters. *Nanotechnology* 2006; **17**, 1558-63.

[11] DH Reneker and I Chun. Nanometre diameter fibres of polymer, produced by electrospinning. *Nanotechnology* 1996; **7**, 216-23.

[12] OO Dosunmu, GG Chase, W Kataphinan and DH Reneker. Electrospinning of polymer

nanofibres from multiple jets on a porous tubular surface. *Nanotechnology* 2006; **17**, 1123-7.
[13] Z Zhou, K Liu, C Lai, L Zhang, J Li, H Hou, DH Reneker and H Fong. Graphitic carbon nanofibers developed from bundles of aligned electrospun polyacrylonitrile nanofibers containing phosphoric acid. *Polymer* 2010; **51**, 2360-7.
[14] X Fang and DH Reneker. DNA fibers by electrospinning. *J. Macromolecular Sci. Phys.* 1997; **B36**, 169-73.
[15] AG MacDiarmid. Nobel lecture: ‘‘Synthetic metals’’: A novel role for organic polymers. *Rev. Mod. Phys.* 2001; **73**, 701-12.
[16] L Jin, T Wang, ML Zhu, MK Leach, YI Naim, JM Corey, ZQ Feng and Q Jiang. Electrospun fibers and tissue engineering. *J. Biomed. Nanotechnols*. 2012; **8**, 1-9.
[17] R Ramaseshan, S Sundarrajan and R Jose. Nanostructured ceramics by electrospinning. *J. Appl. Phys.* 2007; **102**, 111101-17.
[18] AF Spivak and YA Dzenis. Asymptotic decay of radius of a weakly conductive viscous jet in an external electric field. *Appl. Phys. Lett*. 1998; **73**, 3067-9.
[19] AF Spivak, YA Dzenis and DH Reneker. A model of steady state jet in the electrospinning process. *Mech. Res. Commun*. 2000; **27**, 37-42.
[20] MM Hohman, M Shin, G Rutledge and MP Brenner. Electrospinning and electrically forced jets I: stability theory. *Phys. Fluids*. 2001; **13**, 2201-20.
[21] MM Hohman, M Shin, G Rutledge and MP Brenner. Electrospinning and electrically forced jets II: applications. *Phys. Fluids*. 2001; **13**, 2221-36.
[22] JJ Feng. The stretching of an electrified non-Newtonian jet: a model for electrospinning. *Phys. Fluids*. 2002; **14**, 3912-26.
[23] JJ Feng. Stretching of a straight electrically charged viscoelastic jet. *J. Non-Newtonian Fluid Mech*. 2003; **116**, 55-70.
[24] DH Reneker, AL Yarin, H Fong and S Koombhongse. Bending instability of electrically charged liquid jets of polymer solutions in electrospinning. *J. Appl. Phys*. 2000; **87**, 4531-47.
[25] AL Yarin, S Koombhongse and DH Reneker. On bending instability in electrospinning of nanofibers. *J. Appl. Phys.* 2001; **89**, 3018-26.
[26] SA Theron, AL Yarin, E Zussman and E Kroll. Multiple jets in electrospinning: experiment and modeling. *Polymer* 2005; **46**, 2889-99.
[27] CP Carroll and YL Joo. Discretized modeling of electrically driven viscoelastic jets in the initial stage of electrospinning. *J. Appl. Phys.* 2011; **109**, 094315-9.
[28] Y Wu, JY Yu, JH He and YQ Wan. Controlling stability of the electrospun fiber by magnetic field. *Chao. Solit. Fract.* 2006; **32**, 5-7.
[29] L Xu, Y Wu and Y Nawaza. Numerical study of magnetic electrospinning processes. *Comput. Math. Appl.* 2011; **61**, 2116-9.
[30] D Li and Y Xia. Electrospinning of nanofibers: Reinventing the wheel? *Adv. Mater*. 2004; **16**, 1151-70.
[31] WK Son, JH Youk, TS Lee and WH Park. The effects of solution properties and polyelectrolyte on electrospinning of ultrafine poly(ethylene oxide) fibres. *Polymer* 2004; **45**, 2959-66.
[32] WK Son, JH Youk, TS Lee and WH Park. Electrospinning of ultrafine cellulose acetate fibres: Studies of a new solvent system and deacetylation of ultrafine cellulose acetate fibres. *J. Polym. Sci. Part B: Polym. Phys.* 2004; **42**, 5-11.
[33] H Fong, I Chun and DH Reneker. Beaded nanofibers formed during electrospinning. *Polymer* 1999; **40**, 4585-92.
[34] L Wannatong, A Sirivat and P Supaphol. Effects of solvents on electrospun polymeric fibres: Preliminary study on polystyrene. *Polym. Int.* 2004; **53**, 1851-9.
[35] ZM Huang, YZ Zhang, M Kotaki and S Ramakrishna. A review on polymer nanofibers by electrospinning and their applications in nanocomposites. *Compos. Sci. Technol.* 2003; **63**, 2223-53.
[36] A Koski, K Yim and S Shivkumar. Effect of molecular weight on fibrous PVA produced by electrospinning. *Mater. Lett.* 2004; **58**, 493-7.
[37] D Rodoplu and M Mutlu. Effects of electrospinning setup and process parameters on nanofiber morphology intended for the modification of quartz crystal microbalance surfaces. *J. Eng. Fiber. Fabr*. 2012; **2**, 118-23.

[38] SA Theron, E Zussman, AL Yarin. Experimental investigation of the governing parameters in the electrospinning of polymer solutions. *Polymer 2004*; **45**, 2017-30.
[39] SD Vrieze, TV Camp, A Nelvig, B Hagstrom, P Westbroek and KD Clerck. The effect of temperature and humidity on electrospinning. *J. Mater. Sci*. 2009; **44**, 1357-62.
[40] C Wang, HS Chien, CH Hsu, YC Wang, CT Wang and HA Lu. Electrospinning of polyacrylonitrile solutions at elevated temperatures. *Macromolecules* 2007; **40**, 7973-83.
[41] CJ Thompson, GG Chase, AL Yarin and DH Reneker. Effects of parameters on nanofiber diameter determined from electrospinning model. *Polymer* 2007; **48**, 6913-22.
[42] JH He, L Xu, Y Wu and Y Liu. Review mathematical models for continuous electrospun nanofibers and electrospun nanoporous microspheres. *Polym. Int*. 2007; **56**, 1323-9.
[43] MS El Naschie. Nanotechnology for the developing world. *Chao. Solit. Fract*. 2006; **30**, 769-73.
[44] MS El Naschie. The Concepts of E Infinity: An elementary introduction to the Cantorian-fractal theory of quantum physics. *Chao. Solit. Fract.* 2004; **22**, 495-511.
[45] MS El Naschie. Topics in the mathematical physics of E-infinity theory. *Chao. Solit. Fract.* 2006; **30**, 656-63.